



Synthesis, Characterization and Antimicrobial Activity of a Tridentate Hydrazone-hydrazone Ligand Derived from 2-Pyridinecarboxaldehyde and 4-Hydroxybenzohydrazide and Its Co(II) and Zn(II) Complexes

*Abubakar Muhammad Jabbi and Habu Nuhu Aliyu

Department of Pure and Applied Chemistry, Bayero University, P. M. B. 3011, Kano, Nigeria.

*Corresponding authors' email: abubakarmuhammadjabbi@gmail.com

ABSTRACT

A hydrazone-hydrazone ligand was synthesized through the condensation of 2-pyridinecarboxaldehyde and 4-hydroxybenzohydrazide. Its corresponding Co(II) and Zn(II) complexes were prepared and characterized by solubility, melting point and decomposition temperature, elemental analysis, molar conductance, magnetic susceptibility, FTIR, and UV-Vis spectroscopic techniques. Analytical and spectroscopic data confirmed the formation of neutral complexes $[\text{Co}(\text{L})\text{Cl}_2(\text{H}_2\text{O})] \cdot \text{H}_2\text{O}$ and $[\text{Zn}(\text{L})\text{Cl}_2] \cdot \text{H}_2\text{O}$. The IR spectral data of the ligand showed a band at 1648cm^{-1} which were assigned to hydrazide carbonyl ($\text{C}=\text{O}$) this same band was observed to shift to lower frequencies $1635, 1633\text{cm}^{-1}$, after complexation. Another band appeared at 1560cm^{-1} assigned to azomethine $\nu(\text{C}=\text{N})$ and the same band was observed to shift to higher frequencies 1600cm^{-1} and 1611cm^{-1} in the complexes, suggesting coordination of the ligand with the respective metal(II) ions. Other peaks appeared at $608, 577; 508, 551\text{cm}^{-1}$ which are attributed to $\nu(\text{M}-\text{N})$ and $\nu(\text{M}-\text{O})$ respectively, showing that the ligand coordinated in a tridentate manner through hydrazide oxygen, azomethine nitrogen and pyridyl nitrogen. The magnetic moment 4.58 BM of Co(II) suggested its paramagnetic nature, while the value for the Zn(II) complex suggested its diamagnetic nature (0 BM). Molar conductance values 11.58 and $2.70\Omega^{-1}\text{cm}^2\text{mol}^{-1}$ confirmed the neutral nature of both complexes. The result of the antimicrobial showed that the hydrazone-hydrazone ligand itself possessed inherent antifungal properties against *Candida albicans*, *Tinea rubrum* and *Tinea pendis* that may be diminished rather than enhanced by metal coordination. This contrasted with the antibacterial results for tested bacteria *Staphylococcus aureus*, *Escherichia coli* and *Pseudomonas ariginosa* where metal complexation generally improved the activity.

Received: 11 March 2026

Accepted: 05 May 2026

Published: 16 June 2026

Keywords: Tridentate hydrazone-hydrazone, Antimicrobial, Metal(II) Complexes

INTRODUCTION

The challenge of antimicrobial resistance (AMR) represented one of the most pressing concerns confronting contemporary medicine (Mohanty *et al.*, 2021). Pathogenic bacteria have evolved sophisticated resistance mechanisms that enable them to evade the effects of conventional antibiotics (Munita & Arias, 2016). The World Health Organization has classified antimicrobial resistance among the most significant threats to global public health in the 21st century. Furthermore, AMR affected countries in all region and at all income levels, and impose substantial economic burdens through prolonged hospitalizations and elevated healthcare expenditures (Munita & Arias, 2016). These circumstances underscore the critical necessity for developing novel antimicrobial agents. Within this context, hydrazone-hydrazone have attracted sustained scientific interest over several decades (Vineetha *et al.*, 2019; Popiolek, 2017, 2021). These compounds are typically synthesized through condensation reactions between aldehydes or ketones and hydrazides (Czyzewska *et al.*, 2024). The pharmacological relevance of hydrazone-hydrazone stems from their diverse biological properties, which include antibacterial, anticancer (Aliyu and Sani, 2012; Saliyan *et al.*, 2018), antifungal (Cordeiro *et al.*, 2016), and antitubercular activities (Teneva *et al.*, 2023). Notably, several pharmaceuticals currently available on the market, including nitrofurazone, furazolidone, and nitrofurantoin, incorporate the hydrazone scaffold (Popiolek, 2017, 2021; Czyzewska *et al.*, 2024).

Beyond their pharmaceutical applications, hydrazones serve as valuable intermediates in organic synthesis and function as versatile ligands in coordination chemistry (Czyzewska *et al.*, 2024; Tafere *et al.*, 2025). This coordination capability has opened promising avenues for developing metal-based therapeutic agents with potentially enhanced biological profiles. The biological activity of metal complexes arises from the combined contributions of both the organic ligand and the metal center, often resulting in a synergistic effect that surpasses the activity of the ligand alone (Tafere *et al.*, 2025; Leszek *et al.*, 2017). In hydrazone complexes, coordination typically occurs through the imine nitrogen, the amide oxygen, and an additional donor atom which gives rise to tridentate coordination geometries (Bikas *et al.*, 2017; Mathew *et al.*, 2011; Aboafia *et al.*, 2018). Among the various transition metals explored, complexes formed with Cu(II), Ni(II), Cu(II), and Zn(II) have attracted considerable attention due to their promising biological profiles (Wu *et al.*, 2024; Qin *et al.*, 2016; Burgos-López *et al.*, 2022). The scientific literature consistently demonstrates that complexation can significantly enhance a compound's therapeutic potential, improving antimicrobial, anticancer, and anti-inflammatory activities (Kumaret *et al.*, 2025). Additionally, the antibacterial mechanism of certain metal complexes may involve disruption of DNA gyrase enzyme critical for bacterial DNA replication and transcription (Kumaret *et al.*, 2025; Mohler *et al.*, 2017).

Among the metals investigated, Co(II) and Zn(II) complexes have emerged as particularly compelling candidates (Eben & Imlay, 2023). The potential of metal-based strategies to enhance antibiotic efficacy has been the subject of extensive investigation, with studies confirming that complexation with transition metals represented a promising avenue for discovering novel antimicrobial agents (Mohler *et al.*, 2017; Jabbi *et al.*, 2020). This study aims to assess the antimicrobial activity of these newly obtained Co(II) and Zn(II) complexes and how complexation enhanced activity relative to the parent ligands, consistent with trends reported in the literature.

MATERIALS AND METHODS

Chemicals, Reagents and Apparatus

All of the glassware used in this work was thoroughly cleaned. Following a two to three hour soak in a strong nitric acid solution, they were rinsed three times with distilled water before being dried in an oven set to 110°C. All of the reagents were Analytical grade and were used without further purification. On a College B154 Metler Toledo electric balance, all weighing was done. Stuart S.MP 10 melting point apparatus was used to measure melting point and decomposition temperatures. The drying oven model DHO-9053A was used to determine the amount of hydration.

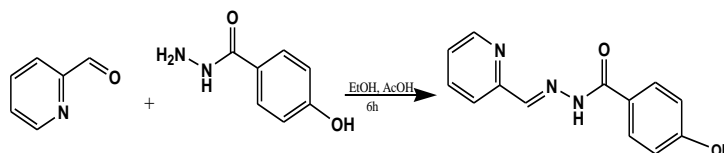


Figure 1: Synthesis of the Hydrazone-Hydrazone Ligand

Complexes

The metal(II) complexes of hydrazone-hydrazone ligands L were prepared by dissolving 10 cm³ of respective metal(II) chlorides of CoCl₂·6H₂O and ZnCl₂ (0.0050 mol) in a hot ethanolic solution of the ligand (0.0050 mol) in 25 cm³ absolute ethanol. 2 - 3 drops of glacial acetic acid were added to the reaction mixture and the mixture was stirred at room temperature for 30 minutes. The subsequent solution was refluxed for 6 hours, after which the mixture was cooled to room temperature. The precipitated complex is collected by filtration, washed with hot ethanol and cold diethylether, and dried under vacuum over phosphorus pentoxide to constant weight for further characterization (Yield: 72%).

RESULTS AND DISCUSSION

Physical Properties of the ligand (L) and its Metal(II) Complexes

The hydrazone-hydrazone ligand was synthesized in good yield (75%) as an off-white through condensation of 4-hydroxybenzohydrazide and 2-pyridinecarboxaldehyde. The Co(II) as brown colour and Zn(II) as cream colour complexes were prepared in 65% and 72% yield respectively, by reaction

Agilent Technologies' Carry 630 FT-IR spectrophotometer was used to measure FT-IR spectra in the 400 - 4000 cm⁻¹ range. Using a Bulk Scientific VGP 210 Atomic Absorption Spectrophotometer, the metal content of each compound was calculated. The elemental analysis was performed using a CE instruments (thermal) EA1110 elements analyser at OEA Labs in Callington, United Kingdom. Utilizing the conductivity meter DDS-307, Jenway, electrical conductivity measurements were also performed. At room temperature, magnetic measurement balance Sherwood Scientific MK 01 model was used to assess magnetic susceptibility.

Synthesis of the Hydrazone-Hydrazone Ligand

The hydrazone-hydrazone ligand L was prepared by condensation of equimolar amounts of 2-pyridinecarboxaldehyde (30 mmol, 2.85 cm³) and 4-hydroxybenzohydrazide (30 mmol, 4.56 g) in ethanol (40 cm³). 2 - 3 drops of glacial acetic acid were added to the reaction mixture. The mixture was stirred at room temperature for 30 minutes and then refluxed for 6 hours. After cooling to ambient temperature, the off-white precipitate formed was collected by filtration, washed with hot ethanol followed by cold diethylether, then cooled at room temperature and dried in a vacuum over calcium chloride (Yield: 75%).

of the ligand with the corresponding metal chlorides in ethanol. The melting points of the hydrazone-hydrazone ligand and decomposition temperatures of the Co(II) and Zn(II) complexes recorded were 218°C, 270°C, and 298 °C respectively.

These figures are relatively high indicating that they are stable compounds. The high decomposition temperatures of the complexes suggested a good chelating effect of the respective ligands, which results in the formation of more stable complexes than do an equivalent number of related monodentate ligands. The molar conductivity values of the complexes in DMSO (10⁻³ M) were found to be 11.58 and 2.70 Ω⁻¹cm²mol⁻¹ for the Co(II) and Zn(II) complexes, respectively.

These low values indicated their non-electrolytic nature, suggesting that the chloride ions were coordinated to the metal centers rather than being free counterions. Co(II) complex was paramagnetic showing a μ_{eff} of 4.58 B.M., characteristic of high-spin Co(II) with three unpaired electrons and significant orbital contribution in an octahedral environment while Zn(II) complex is diamagnetic with a μ_{eff} of 0 B.M., as anticipated for its closed-shell d¹⁰ configuration.

Table 1: Physical Properties of the Ligand (L) and its Metal (II) Complexes

Compounds	Colour	% Yield	Am (Ω ⁻¹ cm ² mol ⁻¹)	M.P. (°C)	μ _{eff} (BM)	S.C. (Ω ⁻¹ cm ⁻¹) x 10 ⁻¹
Ligand (L)	Off-white	75	-	218	-	-
[Co(L)Cl ₂ (H ₂ O)].H ₂ O	Brown	65	11.58	270	4.58	312.09
[Zn(L)Cl ₂].H ₂ O	Cream	72	2.70	298	0	79.21

Key: L = C₁₃H₁₁N₃O₂, Am: Molar Conductance, M.P.: Melting Point, S.C.: Specific Conductance

Solubility Test

The ligand (L) was soluble in ethanol, methanol, DMSO and DMF, but slightly soluble or insoluble in some organic solvent on metal complexation. The complexes Co(II) and

Zn(II) were insoluble in water, acetonitrile, and n-hexane, while maintaining high solubility in DMSO and DMF, consistent with the strong coordinating ability and high polarity of these solvents.

Table 2: Solubility Test of the Ligand (L) and its Metal(II) Complexes

Compound	H ₂ O	EtOH	MeOH	ACN	Ether	DMSO	DMF	n-Hex
Ligand (L)	IS	S	S	IS	IS	S	S	IS
[Co(L)Cl ₂ (H ₂ O)].H ₂ O	IS	SS	SS	IS	IS	S	S	IS
[Zn(L)Cl ₂].H ₂ O	IS	SS	SS	IS	IS	S	S	IS

Key: S = Soluble, SS = Slightly Soluble and IS = Insoluble, L = C₁₃H₁₁N₃O₂

FTIR Analysis

The IR spectral data confirmed successful complexation by the shift in the azomethine $\nu(\text{C}=\text{N})$ stretching frequency from 1560 cm^{-1} in the ligand to 1600 and 1611 cm^{-1} in Co(II), and Zn(II) respectively, indicating coordination through the imine nitrogen. The IR spectral data of the ligand showed a band at 1648 cm^{-1} which were assigned to hydrazide carbonyl $\nu(\text{C}=\text{O})$ this same band was observed to shift to lower frequencies

1635, 1633 cm^{-1} , after complexation. Furthermore, the appearance of new bands in the 595 and 577 cm^{-1} and 567 - 551 cm^{-1} regions, assigned to $\nu(\text{M}-\text{N})$ and $\nu(\text{M}-\text{O})$ vibrations respectively, confirmed bonding through the pyridine nitrogen and carbonyl oxygen atoms. Broad band at 3460 cm^{-1} for the Co(II) complexes verified the presence of coordinated water.

Table 3: IR Spectral Data (cm^{-1}) for the Ligand and its Metal(II) Complexes

Compounds	$\nu(\text{N}-\text{H})$	$\nu(\text{O}-\text{H})$	$\nu(\text{C}=\text{O})$	$\nu(\text{C}=\text{N})\text{hyd}$	$\nu(\text{M}-\text{O})$	$\nu(\text{M}-\text{N})$
Ligand (L)	3056	3212	1648	1560	-	-
[Co(L)Cl ₂ (H ₂ O)].H ₂ O	3045	3460	1635	1600	567	595
[Zn(L)Cl ₂].H ₂ O	3074	3301	1633	1611	551	577

Key: L = C₁₃H₁₁N₃O₂

Determination of Water of Crystallization

The weight loss percentages of the metal(II) complexes indicated the loss of one lattice water molecule from the

Co(II) 4.43% and Zn(II) 4.55%, confirming their formulated structures as monohydrates validating the hydrated formulations of these compounds.

Table 4: Determination of Water of Hydration of Hydrazone-Hydrazone Ligand(L) Complexes

Compound	Weight loss (g)	Percentage (%)
[Co(L)Cl ₂ (H ₂ O)].H ₂ O	0.00885	4.425
[Zn(L)Cl ₂].H ₂ O	0.00911	4.554

Key: L = C₁₃H₁₁N₃O₂

UV-Visible Spectral Data

The UV-visible spectral data revealed key electronic transitions that supported metal coordination and provided geometric insights. The ligand showed a single $\pi \rightarrow \pi^*$ transition at 230 nm, while all metal complexes displayed this band with minor shifts, indicating perturbation of the ligand's

electronic structure on coordination. More significantly, a new absorption band appears at 245 and 230 nm and 335 and 340 nm in the complexes, assigned to $\pi \rightarrow \pi^*$ and $n \rightarrow \pi^*$ transition providing optical confirmation of imine nitrogen bonding to the metal center.

Table 5: UV-Visible Spectral Data for the Hydrazone-Hydrazone Ligand(L) and its Complexes

Compound	$\pi - \pi^*$ transition (nm)	$n - \pi^*$ transition (nm)
Ligand (L)	230 (3.994)	-
[Co(L)Cl ₂ (H ₂ O)].H ₂ O	245 (3.657)	335 (3.748)
[Zn(L)Cl ₂].H ₂ O	230 (3.216)	340 (2.986)

Key: L = C₁₃H₁₁N₃O₂

Elemental Analysis

The elemental analysis data confirmed the chemical compositions for the ligand and its metal complexes. The found percentages of C H N for the ligand is in agreement

with its formula (C₁₃H₁₁N₃O₂) verifying its purity. The agreement between found and calculated values for the metal complexes with C N H validated the proposed molecular formulae derived from spectroscopic studies.

Table 6: Elemental Analysis Data for Ligand and its Metal(II) Complexes

Compound	F. Wt.	% Found (Calculated)		
		C	H	N
Ligand (L)	241.25	64.81(64.73)	4.60(4.62)	17.48(17.38)
[Co(L)Cl ₂ (H ₂ O)].H ₂ O	389.84	40.65(40.70)	3.94(3.81)	10.95(10.88)
[Zn(L)Cl ₂].H ₂ O	339.24	39.82(39.87)	2.27(2.24)	10.52(10.70)

Key: L = C₁₃H₁₁N₃O₂, F.Wt. = Formula Weight

Antibacterial Activity Test

The ligand showed moderate activity against all three tested bacterial strains, with inhibition zones ranging from 11 - 19 mm across different concentrations, exhibiting the strongest

effect against *E. coli*. On complexation, most metal complexes displayed enhanced antibacterial activity compared to the ligand, with the zinc(II) complex showing notable activity against *E. coli*. All compounds demonstrated

clear dose-dependent responses, with larger inhibition zones at higher concentrations. While none of the synthesized compounds surpassed the potency of the standard antibiotic amoxicillin 24 - 31 mm zones, Co(II) derivative exhibited

promising antimicrobial profiles that warranted further investigation. This data supported the hypothesis that metal coordination can significantly enhance the biological activity of hydrazone-hydrazone ligands.

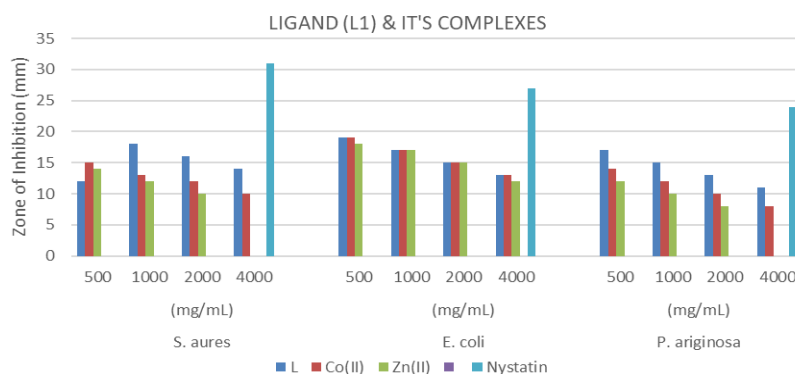


Figure 1: Graphical Representation of Antibacterial Activity Result of the Ligand and its Complexes

Table 7: Antibacterial Activity Test on the Hydrazone-Hydrazone Ligand and its Complexes

Compound	Conc. ($\mu\text{g/mL}$)	Bacterial Inhibition Zones (mm)		
		<i>S. aureus</i> (mm)	<i>E. coli</i> (mm)	<i>P. ariginosa</i> (mm)
Ligand (L)	4000	12	19	17
	2000	18	17	15
	1000	16	15	13
	500	14	13	11
[Co(L)Cl ₂ (H ₂ O)].H ₂ O	4000	15	19	14
	2000	13	17	12
	1000	12	15	10
	500	10	13	8
[Zn(L)Cl ₂].H ₂ O	4000	14	18	12
	2000	12	17	10
	1000	10	15	08
	500	00	12	00
Amoxicillin (125 $\mu\text{g/mL}$)		31	27	24

Key: L = $\text{C}_{13}\text{H}_{11}\text{N}_3\text{O}_2$, Conc. = Concentration, *S. aureus* = *Staphylococcus aureus*, *E. coli* = *Escherichia coli*, *P. ariginosa* = *Pseudomonas ariginosa*

Antibacterial Activity Test

The ligand demonstrated the strongest overall antifungal activity, particularly against *Candida albicans* with inhibition zones reaching 22 mm at the highest concentration, and showed good activity against *Tinea pedis* as well. On metal complexation, the antifungal potency generally decreased compared to the free ligand, with most complexes showing moderate to weak activity. The Zn(II) complex showed selective potency against *Tinea rubrum*. The Co(II) complex demonstrated the weakest overall antifungal profile. All compounds displayed clear concentration-dependent activity,

with larger inhibition zones at higher concentrations. While none of the compounds approached the potency of the standard antifungal Nystatin 25 - 33 mm zones, the ligand's notable activity against *C. albicans* suggested that the hydrazone-hydrazone scaffold itself possessed inherent antifungal properties that may be diminished rather than enhanced by metal coordination in this series. This contrasted with the antibacterial results where metal complexation generally improved activity.

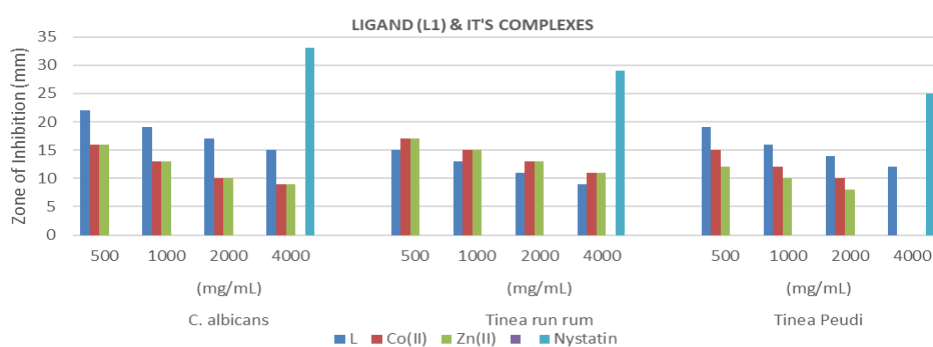


Figure 2: Graphical Representation of Antifungal Activity Result of the Ligand and its Complexes

Table 8: Antifungal Activity Test on the Hydrazone-Hydrazone Ligand and its Complexes

Compound	Conc. ($\mu\text{g/mL}$)	Fungal Inhibition Zones (mm)		
		<i>C. albicans</i> (mm)	<i>Tinea rub rum</i> (mm)	<i>Tinea Pedis</i> (mm)
Ligand (L)	4000	22	15	19
	2000	19	13	16
	1000	17	11	14
	500	15	09	12
[Co(L)Cl ₂ (H ₂ O)].H ₂ O	4000	16	17	15
	2000	13	15	12
	1000	10	13	10
	500	9	11	00
[Zn(L)Cl ₂].H ₂ O	4000	16	18	12
	2000	14	16	10
	1000	12	14	08
	500	10	12	00
Nystatin (125 $\mu\text{g/mL}$)		33	29	25

Key: L = C₁₃H₁₁N₃O₂, Conc. = Concentration, *C. Albicans* = *Candida Albicans*

CONCLUSION

Tridentate hydrazone-hydrazone ligand derived from 4-hydroxybenzohydrazide and 2-pyridinecarboxaldehyde was successfully synthesized and characterized. Its Co(II) and Zn(II) complexes were prepared and thoroughly investigated using solubility, melting point and decomposition temperature, elemental analysis, molar conductance, magnetic susceptibility, FTIR, and UV-Vis spectroscopic techniques. The physicochemical characterization revealed distinct coordination behaviors for the two metal ions Co(II) and Zn(II). The Co(II) complex adopted an octahedral geometry with the ligand acting as a neutral tridentate NNO

donor, coordinated through amide oxygen, azomethine nitrogen, and pyridyl nitrogen, with the remaining sites occupied by chloride and water molecules. The Zn(II) complex exhibited distorted square pyramidal geometry with the ligand coordinating through carbonyl oxygen, azomethine nitrogen, and pyridyl nitrogen, with chloride completing the coordination sphere. The result of the antimicrobial showed that the hydrazone-hydrazone ligand itself possessed inherent antifungal properties that may be diminished rather than enhanced by metal coordination in this series. This contrasted with the antibacterial results where metal complexation generally improved activity.

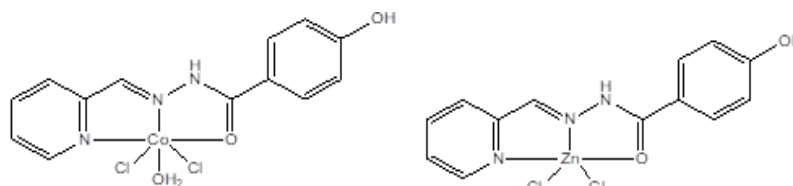


Figure 2: Proposed Structures of the Metal(II) Complexes

REFERENCES

- Aboafia, S.A., Elsayed, S.A., El-Sayed, A.K.A. (2018). El-Hendawy, A.M. New transition metal complexes of 2,4-dihydroxybenzaldehyde benzoylhydrazone Schiff base (H 2 dbbh): Synthesis, spectroscopic characterization, DNA binding/cleavage and antioxidant activity. *Journal of Molecular Structure* 1158, 39–50. Doi: <http://doi.org/10.1016/molstruc.2018.01.008>
- Aliyu, H. N. and Sani, U. (2012). Synthesis, Characterization and Biological Activity of Manganese(II), Iron(II), Cobalt(II), Nickel(II) and Copper(II) Schiff Base Complexes against multidrug Resistant Bacterial and Fungal Pathogens. *International Research Journal of Pharmacy and Pharmacology (I-ISSN 2251-0176)*. 2(2): 040-044.
- Bikas, R., Ghorbanloo, M., Sasani, R., Pantenburg, I., Meyer, G. (2011). Mn(II) complexes of hydrazone based NNO-donor ligands and their catalytic activity in the oxidation of olefins. *Journal of Coordination Chemistry*, 70, 819 - 830. Doi: <http://doi.org/10.1080/00958972.2017.1281918>
- Burgos-López, Y., Balsa, L.M.; Piro, O.E.; León, I.E.; García-Tojal, J.; Echeverría, G.A.; González-Baró, A.C., Parajón-Costa, B.S. (2022). Tridentate acylhydrazone copper(II) complexes with heterocyclic bases as coligands. Synthesis, spectroscopic studies, crystal structure and cytotoxicity assays. *Polyherdon*. 213, 115621. Doi: <http://doi.org/10.1016/j.poly.2021.115621>
- Cordeiro, R.d.A., de Melo, C.V., Marques, F.J., Serpa, R., Evangelista, A.J., Caetano, E.P.; Mafezoli, J., Oliveira, M.d.C.F.d., da Silva, M.R., Bandeira, T.d.J.P.G., (2016). Synthesis and in vitro antifungal activity of isoniazid-derived hydrazones against *Coccidioides posadasii*. *Microbial Pathogenesis* 98, 1 - 5. Doi: <http://doi.org/10.1016/j.micpath.2016.06.022>
- Czyżewska, I.; Mazur, L., Biernasiuk, A., Hordyjewska, A., Popiołek, L.(2024). Synthesis, Structural Properties and Biological Activities of Novel Hydrazones of 2-, 3-, 4-Iodobenzoic Acid. *Molecules*. 29, 3814. Doi: <http://doi.org/10.3390/molecules29163614>
- Czyżewska, I., Mazur, L., Biernasiuk, A., Hordyjewska, A., Popiołek, L. (2025). Novel derivatives of nicotinic acid: Synthesis, crystal structure, antimicrobial activity and cytotoxicity. *Chemistry and Biodiversity*. 22, e202500264. Doi: <http://doi.org/10.1002/cbdv.202500264>
- Czyżewska, I., Mazur, L., Popiołek, L. (2024). Transition metal complexes of hydrazones as potential antimicrobial and anticancer agents: A short review. *Chemical Biology and*

- Drug Design.* 104, e14590. Doi: <http://doi.org/10.1111/cbdd.14590>
- Eben, S.S. Imlay, J.A. (2023). Excess copper catalyzes protein disulfide bond formation in the bacterial periplasm but not in the cytoplasm. *Molecular Microbiology* 119, 423–438. Doi: <http://doi.org/10.1111/mmi.15032>
- Jabbi, A. M., Aliyu, H. N., Isyaku, S. and Kabir, A. M. (2020) Preparation, Characterization and Antimicrobial Studies of Mn(II) and Fe(II) Complexes with Schiff Base Ligand Derived from 2-aminophenol and 3-formyl-2-hydroxy-6-methoxyquinoline. *Open Journal of Inorganic Chemistry*, 10(2), 15-24. Doi: <https://doi.org/10.4236/ojic.2020.102003>
- Leszek, J., Trypka, E., Tarasov, V.V., Ashraf, G.M., Aliev, G. (2017). Type 3 diabetes mellitus: A novel implication of Alzheimer's disease. *Curr. Top. Medicinal Chemistry* 17, 1331–1335. Doi: <http://doi.org/10.2174/15680266176660103163403>
- Mathew, N.; Sithambaresan, M., Kurup, M.R. (2011). Spectral studies of copper(II) complexes of tridentate acylhydrazone ligands with heterocyclic compounds as coligands: X-ray crystal structure of one acylhydrazone copper(II) complex. *Spectrochim. Acta A Molecular Biomol. Spectrosc.* 79, 1154 - 1161. Doi: <http://doi.10.1016/j.saa.2011.04.036>
- Meshram, U.P., Pethe, G.B., Yaul, A.R., Khobragade, B.G., Narwade, M.L. (2017). Studies in stability constants of schiff base hydrazone complexes with transition metal ions. Effect of ligand on seed germination. *Russian Journal of Physical Chemistry A*, 91, 1877–1882. Doi: <http://doi.org/10.1134/S0036024417100259>
- Mohanty, H., Pachpute, S., Yadav, R.P. (2021). Mechanism of drug resistance in bacteria: Efflux pump modulation for designing of new antibiotic enhancers. *Folia Microbiol.* 66, 727-739. Doi: <http://doi:10.1007/s12223-021-00910-2>
- Mohler, J.S., Kolmar, T., Synnatschke, K., Hergert, M., Wilson, L.A., Ramu, S., Elliott, A.G., Blaskovich, M.A., Sidjabat, H.E., Paterson, D.L. (2017). Enhancement of antibiotic-activity through complexation with metal ions - Combined ITC, NMR, enzymatic and biological studies. *Journal of Inorganic Biochemistry* 167, 134 - 141. Doi: <http://doi.org/10.1016/j.jinorgbio.2016.11.028>
- Munita, J.M.; Arias, C.A. (2016). Mechanisms of Antibiotic Resistance. *Microbiology Spectr.* 4, 464-473. Doi: <http://doi.10.1128/microbiolspec.VMBF-0016-2015>
- Popiolek, L. (2017). Hydrazone-hydrazones as potential antimicrobial agents: Overview of the literature since 2010. *Medicinal Chemistry Research* 26, 287-301. Doi: <http://doi.10.1007/s00044-016-1756-y>
- Popiolek, L. (2021). Updated information on antimicrobial activity of hydrazone-hydrazones. *International Journal of Molecular Science*, 22, 9389. Doi: <http://doi.org/10.3390/ijms22179389>
- Qin, J., Zhao, S.S., Liu, Y.P., Man, Z.W., Wang, P., Wang, L.N., Xu, Y., Zhu, H.L. (2016) Preparations, characterization, and biological features of mononuclear Cu(II) complexes based on hydrazone ligands. *Bioorganic Medicinal Chemistry Letters* 26, 4925 - 4929. Doi: <http://doi.org/10.1016/j.bmcl.2016.09.015>
- Salian, A.R.; Foro, S.; Gowda, B.T. (2018). Crystal structures and the Hirshfeld surface analysis of (E)-4-nitro-N'-(o-chloro, o- and p-methyl-benzyl-iden)benzene-sulfonyl-hydrazides. *Acta Crystallogr. Sect. E Crystallographic Communications.* 74, 1710 - 1716. Doi: <http://doi.org/10.1107/S2056989018014500>
- Tafere, D.A.; Gebrezgiabher, M.; Elemo, F.; Sani, T.; Atisme, T.B.; Ashebr, T.G.; Ahmed, I.N. (2025). Hydrazones, hydrazones-based coinage metal complexes, and their biological applications. *RSC Adv.* 15, 6191 - 6207. Doi: <http://doi.org/10.1039/D4RA07794F>
- Tang, D., Kroemer, G., Kang, R. (2024). Targeting cuproplasia and cuproptosis in cancer. *Natural Review Clinical Oncology.* 21, 370 - 388. Doi: <http://doi.org/10.1038/s41571-024-00876-0>
- Kumar, N.; Kaushal, R.; Awasthi, P. (2025). Transition Metal Complexes as Antibacterial Agents: An Overview. *J. Fluoresc.* 24, 1 - 7. Doi: <http://doi.org/10.1007/s10895-025-04313-y>
- Teneva, Y.; Simeonova, R.; Valcheva, V.; Angelova, V.T. (2023). Recent Advances in Anti-Tuberculosis Drug Discovery Based on Hydrazone-Hydrazone and Thiadiazole Derivatives Targeting InhA. *Pharmaceuticals.* 16, 484. Doi: <http://doi.org/10.3390/ph16040484>
- Vineetha, M.C.; Sithambaresan, M.; Nair, Y.S.; Prathapachandra Kurup, M.R. (2019). Structural investigation of discrete solvent protonated vanadium and other transition metal complexes of N'-[(E)-(3-ethoxy-2-hydroxyphenyl)methylidene]benzohydrazide, synthetic, spectroscopic and cytotoxicity studies. *Inorganic Chimica Acta.* 491, 93-104. Doi: <http://doi.10.1016/j.ica.2019.03.040>
- Wu, Y., Wu, D., Lan, K., Li, A., Hou, L., Xu, Y., Gou, Y. (2024). Assessment of Mononuclear/Dinuclear copper acylhydrazone complexes for lung cancer treatment. *Bioorg. Chem.* 144, 107122. Doi: <http://doi.org/10.1016/j.bioorg.2024.107122>

APPENDISES

Figures Showing FT-IR Data For The Ligand and Metal(II) Complexes

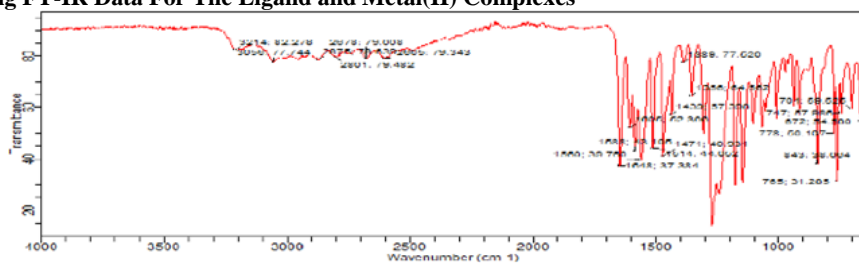


Figure 3: IR Spectrum of Hydrazone-Hydrazone Ligand

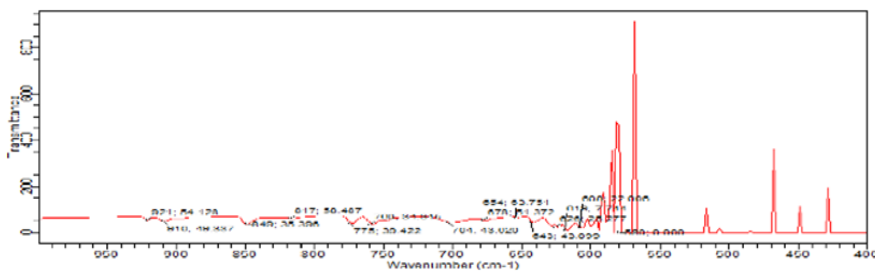


Figure 4: FT-IR Lower Region Spectrum of [Co(L)Cl₂(H₂O)].H₂O Complex

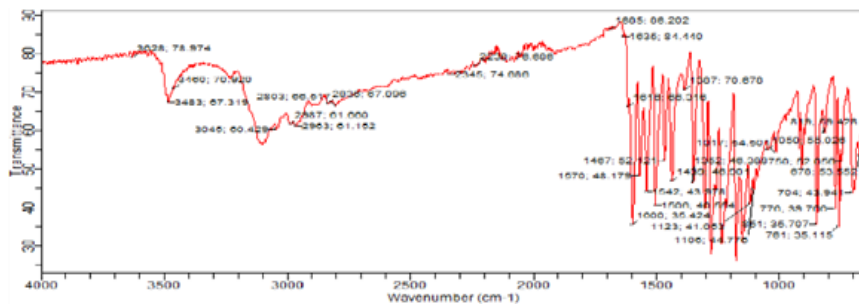


Figure 5: FT-IR Higher Region Spectrum of [Co(L)Cl₂(H₂O)].H₂O Complex

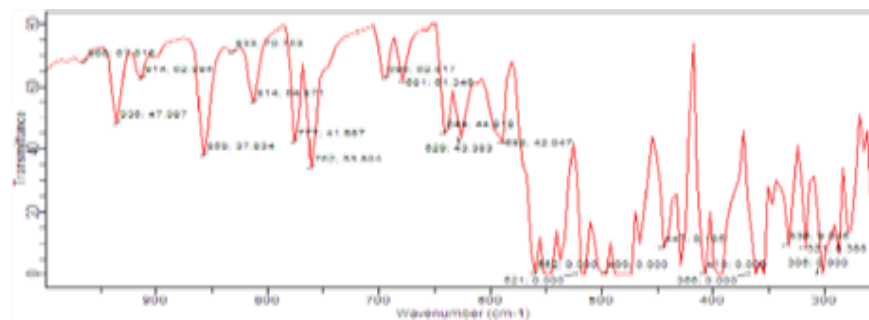


Figure 6: FT-IR Lower Region Spectrum of [Zn(L)Cl₂].H₂O Complex

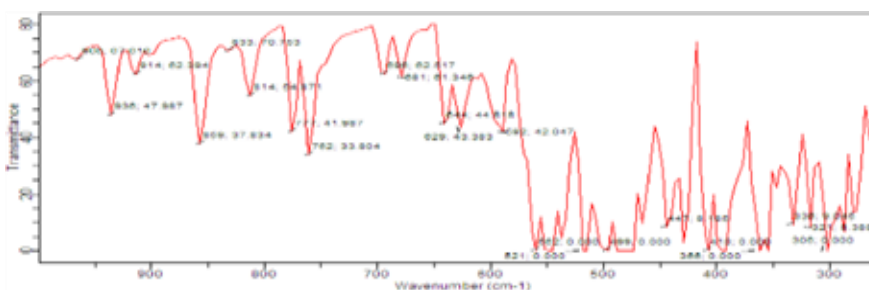


Figure 7: FT-IR Higher Region Spectrum of [Zn(L)Cl₂].H₂O Complex

Figures Showing UV-Visible Data For The Ligand and Metal(II) Complexes

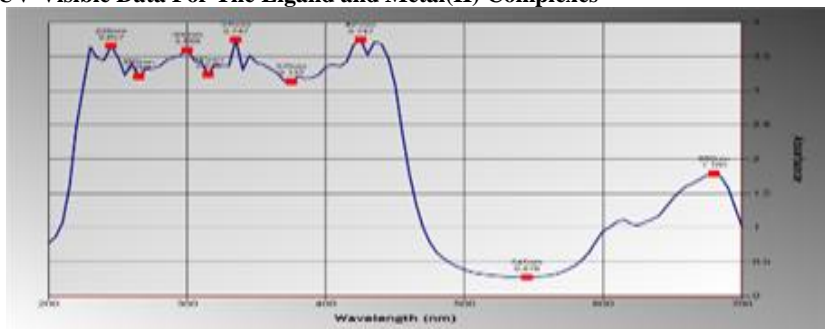


Figure 8: UV-Visible Spectrum of [Co(L)Cl₂(H₂O)].H₂O Complex

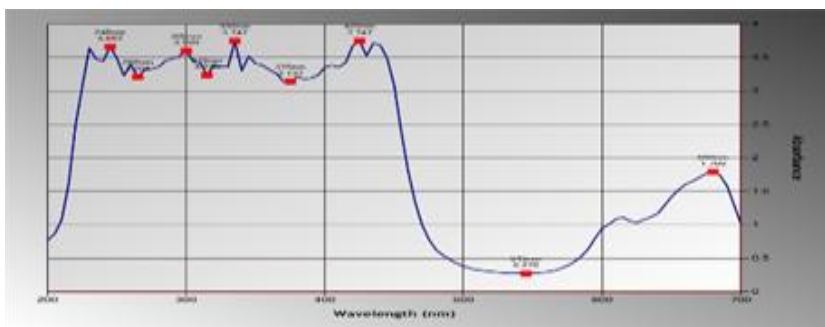


Figure 9: UV-Visible Spectrum of [Zn(L)Cl₂].H₂O Complex



©2026 This is an Open Access article distributed under the terms of the Creative Commons Attribution 4.0 International license viewed via <https://creativecommons.org/licenses/by/4.0/> which permits unrestricted use, distribution, and reproduction in any medium, provided the original work is cited appropriately.